H2Open Journal

H_2Open Journal Vol 6 No 1, 63 doi: 10.2166/h2oj.2023.062

Evaluation of land use/land cover datasets in hydrological modelling using the SWAT model

Sayed Amir Alawi * and Sevinç Özkul

Department of Civil Engineering, Dokuz Eylul University, Doğuş Caddesi, Tinaztepe Campus, Buca, Izmir 35390, Türkiye
*Corresponding author. E-mail: amiralawi2015@gmail.com

SAA, 0000-0003-1188-0763

ABSTRACT

Land use/land cover (LULC) is a key influencer for runoff generation and the estimation of evapotranspiration in the hydrology of watersheds. Therefore, it is essential to use accurate and reliable LULC data in hydrological modelling. Ground-based data deficiencies are a big challenge in most parts of developing countries and remote areas around the globe. The main objective of this research was to evaluate the accuracy of LULC data from two different sources in hydrological modelling using the soil and water assessment tool (SWAT). The first LULC data was prepared by the classification of Landsat 8 satellite imagery, and the second LULC data was extracted from the ESRI 2020 global LULC dataset. The study was conducted on the Kokcha Watershed, a mountainous basin partly covered by permanent snow and glaciers. The accuracy assessment was done based on a comparison between observed river discharge and simulated river flow, utilizing each LULC dataset separately. After calibration and validation of the models, the acquired result was approximately similar and slightly (5.5%) different. However, due to the higher resolution and easily accessible ESRI 2020 dataset, it is recommended to use ESRI 2020 in hydrological modelling using the SWAT model.

Key words: Amu Darya, hydrological modelling, Kokcha Watershed, LULC datasets, SWAT model

HIGHLIGHTS

- Two land use/land cover (LULC) datasets were evaluated to analyse their accuracy.
- The ESRI LULC dataset represents a more accurate result than LULC data, which was prepared by the classification of Landsat 8 satellite images.
- The utilized remote sensing data in this study can be used in hydrological modelling for similar studies in the region.

GRAPHICAL ABSTRACT

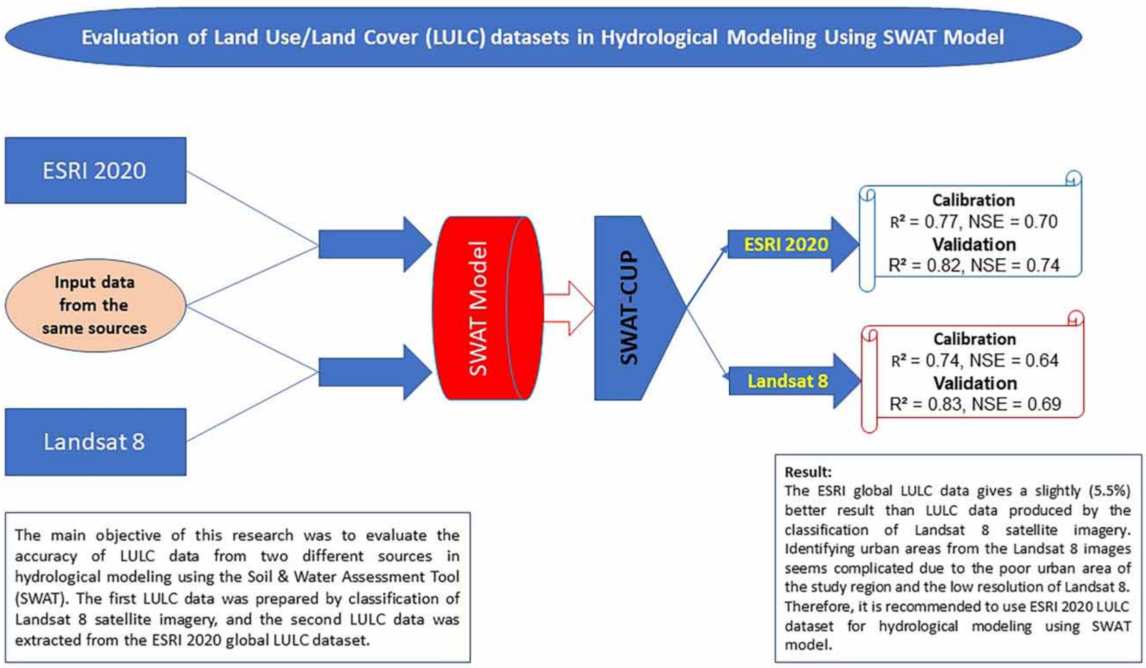

INTRODUCTION

Nowadays, in the changing climate and warming conditions, proper management of water resources, and the design of water infrastructures extremely depend on hydrological modelling. Data deficiencies are a concern for hydrologists and water managers all around the world, particularly in developing countries and remote areas. Hydrological modelling using remotely sensed data is progressing in recent years, especially in data-scarce regions (Li *et al.* 2012). Utilizing remote sensing data helps to 'simulate the impacts of human actions on water resources and assist in the planning and management of river basins' (Almeida *et al.* 2018). Thus, investigating the influence of environmental change on watersheds is as important as the proper utilization of remotely sensed information for hydrological modelling. LULC has a vital role in generating surface flow due to its direct impact on infiltration and evapotranspiration in addition to many factors such as slope, soil types, and weather conditions. According to research carried out in the upper Mara River, Kenya, 97.5% of changes in river flow were caused by LULC change (Mwangi *et al.* 2016). Therefore, while utilizing remotely sensed data, we need to choose it from a reliable source.

Hydrologists and water managers need to use the most updated LULC data in hydrologic calculation and runoff modelling. Remotely sensed data are valuable sources to produce an up-to-date LULC classification (Steinhausen *et al.* 2018 cited by Chaves *et al.* (2020)). Under the effects of climate change, water resources management becomes so sensitive, and the most precise input data should be used in hydrological modelling. Many datasets produce and release global LULC, but their adoption and application need evaluation. Therefore, before using the global LULC data products, it is necessary to evaluate their suitability in the region. Studies have been done to analyse the accuracy of remote sensing data and their application in different regions of the world. For instance, the three global LULC data like the 'Google's dynamic world (DW), European Space Agency (ESA)'s world cover (WC), and ESRI LULC datasets were released in 2020 with strong spatial correspondence' (Venter *et al.* 2022). A study conducted on these three LULC datasets using global ground truth data with a minimum mapping unit of 250 m^2 revealed that the ESRI had the highest overall accuracy (75%) compared with DW (72%) and WC (65%) (Venter *et al.* 2022). When these data products were evaluated 'using the European ground truth data from LUCAS (Land use/cover area frame survey) with a minimum mapping unit of' $<$100 m^2, WC showed the highest accuracy (71%) compared with DW (66%) and ESRI (65%) (Venter *et al.* 2022). The interesting point of this research is the accuracy of ESRI and DW datasets on the global scale, whereas, the WC dataset represented more precision on the European scale. Thus, each LULC dataset can represent a certain precision in some areas, but not for all regions.

The CORINE and Landsat 7 ETM LULC datasets were investigated by Cuceloglu *et al.* (2021) to evaluate their accuracy in the Omerli River Basin of Istanbul. The LULC data were both obtained in the year 2006 and investigated employing the soil and water assessment tool (SWAT) model. The result was quite similar in terms of surface runoff (SF) and actual evapotranspiration; however, different spatial distribution was observed especially in urbanized sub-basins (Cuceloglu *et al.* 2021). A comparison between two satellite images (Landsat 8 and Sentinel 2) was done using the Google Earth Engine (GEE) to evaluate the accuracy of classified LULC data. Application of this research in Kabul City indicated that Sentinel-2 satellite images can produce more precise LULC data than Landsat 8 (Ahady & Kaplan 2022). Four LULC datasets were considered to investigate their accuracy in the Indochina Peninsula as the research area. Among LSV10, GLC_FCS30, ESRI10, and Globeland30, the overall accuracy of LSV10 was detected as the highest (83.25%) and GLC_FCS30 was evaluated as the lowest (72.27%) accurate (Wang *et al.* 2022). Due to variations in the geology and environmental characteristics of regions, utilizing remote sensing data requires investigation and accuracy assessment.

Hydrologic responses against climate and land cover change become so sensible in watersheds that are located in arid regions (Zhou *et al.* 2013; Getachew *et al.* 2021; Serur & Adi 2022 cited by Ahmadi *et al.* (2022)). To have accurate forecasting, researchers and water managers need to investigate the performance of models and datasets. A reliable runoff estimation in hydrological modelling requires developing and applying various techniques to make the models more precise (Althoff *et al.* 2021). In recent years, the SWAT model is one of the most popular tools in hydrological modelling, which widely utilizes in different parts of the world. A study was conducted by Liu *et al.* (2018) to compare the performance of the SWAT model and IHACRES ('Identification of unit Hydrograph and Component flows from Rainfall, Evapotranspiration, and Streamflow') model in streamflow simulation of Naoli Watershed, Northeast China. This study has shown that the SWAT model potentially give better results for hydrological modelling and water resources planning and management. Nilawar & Waikar (2018) used the SWAT model to analyse the effects of climate and land use change on the streamflow and sediment simulation in the Purna River Basin, India. This study revealed that the SWAT model can simulate long-term hydrological processes in the Purna Watershed. Based on a study conducted in the Segura Watershed to analyse the influence of climate change and deforestation, the SWAT model accurately replicated monthly streamflow considering climate and land use change (Senent-Aparicio *et al.* 2018).

Due to the lack of observed data in Afghanistan, utilizing remotely sensed data is the only option for hydrologic calculations and climate change analysis. The vulnerable water resources to climate change in Afghanistan is another issue in addition to many problems, such as data scarcity, non-stable government, and economic problems. Researchers in this country mostly use the LULC data that was prepared by UN-FAO in 1993 and 2003. Whereas, in the past two decades, there were major developments in urban and agricultural lands. To have better control over the water resources of a watershed, researchers need accurate and reliable input data for hydrological modelling. Furthermore, the performance of models in streamflow simulation plays an important role in the hydrological modelling of ungauged watersheds. In recent years, researchers and designers have utilized different hydrological models in various parts of Afghanistan. Among the models, the SWAT model was employed in hydrological modelling at some river basins in the country. For example, the SWAT model was applied in the simulation of SF in the Balkhab River Basin during 2013–2018. The land cover atlas of the Islamic Republic of Afghanistan was used in the hydrological modelling of the Balkhab Watershed, this LULC was prepared by UN-FAO in cooperation with the Ministry of Agriculture, Irrigation and Livestock in the year 2010. The study revealed satisfactory results for all four sub-basins of the Balkhab Catchment (Husainzada & Lee 2021).

Simulation of SF and sediment yield in the Salma Dam's Watershed has been done utilizing the SWAT model and the obtained result was satisfactory (Sediqi *et al.* 2019; Husainzada & Lee 2021). Simulating the discharge in the Helmand River Basin from 1969 to 1979 has been performed using the SWAT model and the model outcome was utilized to evaluate the 1973 agreement of the Helmand River in southern Afghanistan (Hajihosseini *et al.* 2016). Various parts of the country need clarification in the application of remote sensing datasets and hydrologic models. In recent years, studies conducted to address the application of LULC datasets utilizing various methods on some river basins of Afghanistan. However, there are very limited studies to address the application of ESRI 2020 and Landsat 8 datasets in hydrological modelling using the SWAT model in the Kokcha River Basin. Accurate and reliable LULC datasets have not been clarified by evaluating the datasets in the SWAT model. The main objective of this study was to evaluate the accuracy of LULC datasets from different sources in hydrological modelling using the SWAT model. The datasets are ESRI global LULC and Landsat 8 satellite imagery.

MATERIALS AND METHODS

This study was conducted on a mountainous area that is partly covered by permanent snow/ice. All input data in the SWAT model were obtained from remote sensing sources. Two different LULC datasets were investigated in hydrological modelling. The SWAT model was run by using every LULC data separately and the other input data were utilized from the same sources. The model outputs were calibrated and validated based on observed river discharge employing the SWAT-calibration and uncertainty programme (SWAT-CUP) to evaluate the variations between the two models.

Study area

The study area is Kokcha Watershed, a sub-basin of the Amu Darya River Basin, positioned between 35.436°–36.463° latitude and 69.481°–71.652° longitude with a 20,139 km^2 area. Altitudes in the catchment area range between 480 and 6,737 m (Figure 1). Maximum and minimum temperatures in the Kokcha Basin range from 24.5 °C in the summer to −33.0 °C in the winter. Precipitation falls during the winter months of January and February when the air temperature is below 0 °C in the watershed. This is a great advantage of the study area that converts the precipitation into ice and saves them for other seasons to feed the river and supply peak water demand.

Description of the SWAT model

The United States Department of Agriculture (USDA), agriculture research services developed the SWAT model (Arnold *et al.* 1998). It is a hydrological model that is employed to specify the quantity and quality of water and sediment yield (Shivhare *et al.* 2018). The SWAT model is a continuously under-development model that was used around different countries over long periods for modelling large and complex watersheds. 'In the SWAT

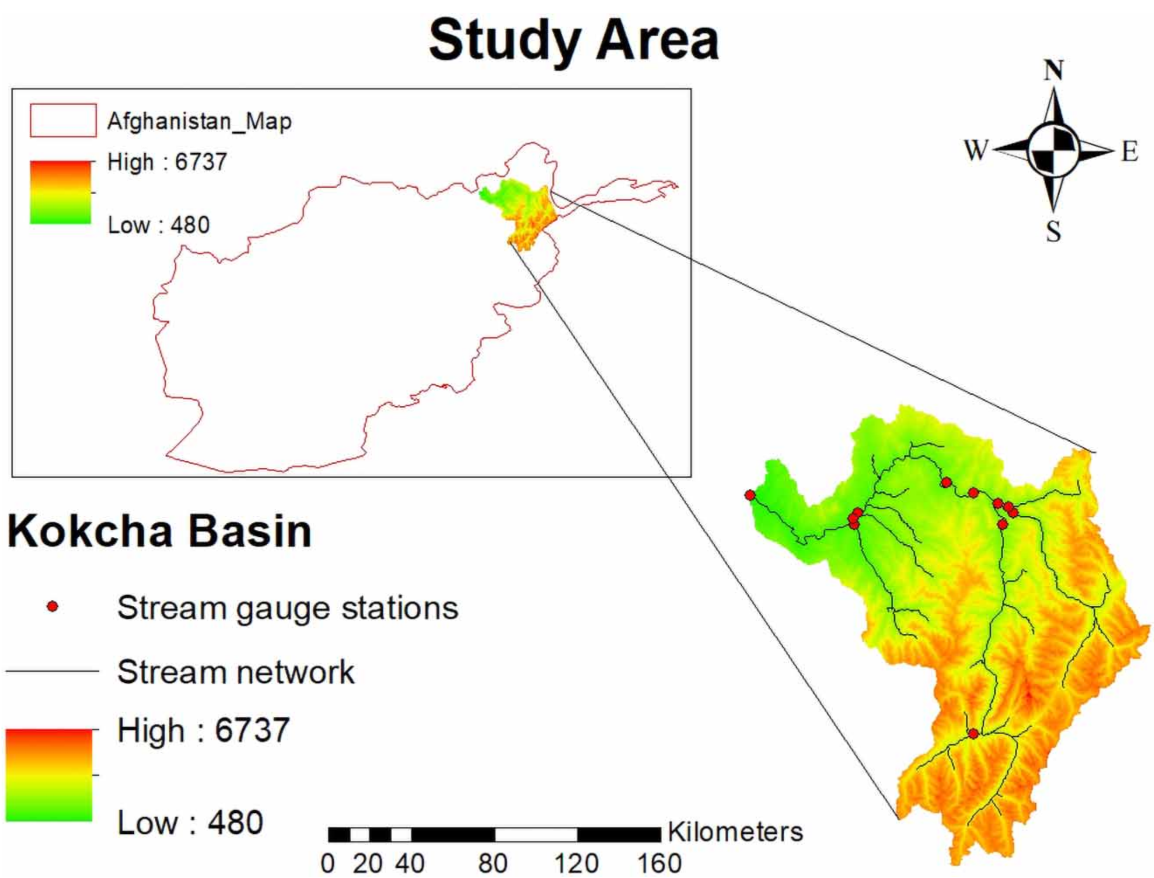

Figure 1 | Location of Kokcha Basin.

model, the basin is subdivided into multiple sub-basins, each sub-basin is divided into hydrological response units (HRUs) that consist of unique homogenous combinations of soil and land use properties' (Arnold *et al.* 2012). The SWAT model utilizes the water balance equation in watershed modelling (Neitsch *et al.* 2011):

$$SW_t = SW_0 + \sum_{i=1}^{i=t} (R_{day} - Q_{surf} - E_a - W_{perc} - Q_{gw}) \tag{1}$$

When R_{day} is the quantity of precipitation (mm/day), t is the time (day), runoff (Q_{surf}) is measured in mm/day, evapotranspiration (E_a) is measured in mm/day, percolation (W_{perc}) is measured in mm/day, and return flow (RF) (Q_{gw}) is measured in mm/day. SW_t and SW_0 are the last and first soil water contents, respectively (Liu *et al.* 2018).

The SWAT model needs spatial data representation like a digital elevation model (DEM), soil map, and the LULC of the watershed. Climate data, including precipitation, maximum and minimum air temperatures, wind speed, solar radiation, and relative humidity in daily or hourly time steps are needed as input data. To simulate potential evapotranspiration (PET), the SWAT model uses the Penman–Monteith, Priestley–Taylor, and Hargreaves methods. In the absence of weather data in modelling, the SWAT model can generate the required climate data. There are two alternative methods to simulate SF using the SWAT model: the Green–Ampt and the USDA's soil conservation service's (SCS)-curve number (CN) methods (USDA 1972; Hallouz *et al.* 2018).

Input data and model setup

For hydrological modelling, the accuracy of input data is the most considered issue for reaching appropriate results. However, ground-based data deficiencies are a big challenge in remote areas and most parts of developing countries. Satellite-based and remotely sensed information is an option to fill the gap of data scarcity in the hydrological modelling of ungauged watersheds (Li *et al.* 2012). In this research, the DEM with 30 m resolution was acquired from the United States Geological Survey (USGS)'s shuttle radar topography mission (STRM) (www.earthexplorer.usgs.gov). The DEM was masked and projected in UTM_N42 using ArcGIS 10.5 to be ready for the SWAT model. The slope and stream network data are derived from DEM with standard flow accumulation. Land use/land cover (LULC) data were obtained from two different sources.

The first LULC data produced by the classification of Landsat 8 OLI/TIRS C1 Level 1 satellite imagery and aerial photographs, with 30 m spatial resolution downloaded considering August 2020. There are five LULC types identified by supervised classification and maximum likelihood method, which are bare ground, snow/ice, urban area, vegetation, and water (Figure 2(a)). The second LULC data was extracted from the ESRI 2020 global LULC dataset that has a 10 m spatial resolution (Figure 2(b)). This high-resolution 'Land cover map was built using European Space Agency (ESA) Sentinel-2 satellite imagery and developed using a new machine learning workflow teaming with the new ESRI Silver Partner Impact Observatory as well as long-time partner Microsoft' (Esri 2021). There are nine types of LULC classes in the area, which are dominated by scrub/shrub

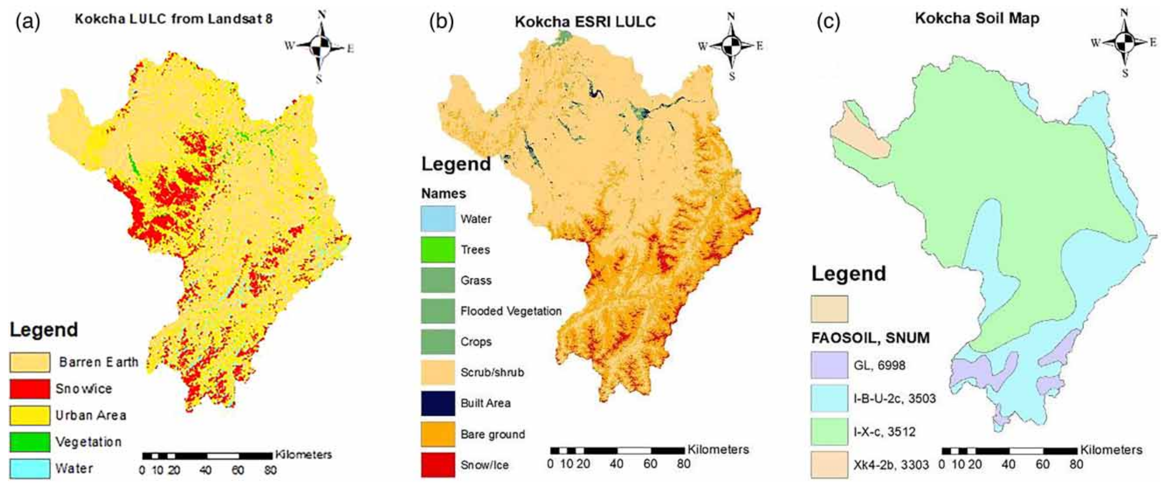

Figure 2 | Kokcha LULC and soil map: (a) Landsat 8 2020; (b) ESRI 2020; and (c) Kokcha soil map.

following the bare ground, snow/ice, crops, built area, water, trees, grasses, and flooded vegetation. Soil data were clipped from UN-FAO global soil map shapefile database and projected in the UTM_N42 projection system using ArcGIS 10.5 to be ready as input data for the SWAT model (Figure 2(c)). There are four types of soils in the Kokcha Watershed coded as I-B-U-2c (Lithosols, Xerosols, Chernozems), I-X-c (Lithosols, Xerosols, Chernozems), Xk4-2b (Calcic Xerosols), and Glacier.

The precipitation data was acquired from tropical rainfall measurement mission (TRMM_3B42) version 7 in a daily time step that has 0.25° × 0.25° spatial resolution. This data product is a result of a collaboration between the NASA and the Japanese Aerospace Exploration Agency (JAXA), which is known as the TRMM multi-satellite precipitation analysis (TMPA) (GES DISC 2015). The first precipitation radar (PR) in space is located in the observatory TRMM, which was launched in 1997 into a nearly circular orbit of around 92.5 min (GES DISC 2015). The TRMM satellite constellation makes use of several satellites, including the PR, TRMM microwave imager (TMI), and visible infrared scanner (VIRS) (Elachi & Van Zyl 2006). The maximum and minimum air temperatures, solar radiation, wind speed, and relative humidity for each of the 10 hydro-meteorological stations that are available in the watershed were obtained from the NASA POWER data collection (https://power.larc.nasa.gov). For local and international data requests, the POWER data archive offers a 0.5 × 0.5-degree resolution (https://data.nasa.gov). The observed monthly streamflow data from 2008 to 2019 was obtained from the water resources department of the National Water Affairs Regulation Authority (NWARA), Afghanistan.

The model simulation was performed from 2008 to 2019 with 2 years (2008 and 2009) warm-up period. In the model setup, the SCS-CN was chosen in runoff estimation, Penman–Monteith method was selected in PET calculation due to its good performance in the region. Also, the model printout was chosen as a monthly time scale. In this study, Hargreaves and Penman–Monteith methods were employed in the PET estimation and the obtained result from the Penman method seems better than the Hargreaves method. Using DEM data and the hydrological analysis tool in ArcGIS software, the SWAT model splits the basin into 25 sub-basins. HRUs affect by a combination of LULC, soil map, and slope of the catchment, there were 464 HRUs defined in the Kokcha Watershed using Landsat 8 LULC data, whereas utilizing ESRI LULC data, 25 sub-basins and 318 HRUs were created, although the setting for slope, soil, and LULC map were considered the same for each of the model setups. Soil and slope are not more effective in the creation of HRUs due to not being variable over short periods, but LULC data is the main cause of differentiation in generating HRUs.

The SWAT-CUP was employed for the calibration of parameters. This application was created to analyse uncertainty and performs calibration and validation of the SWAT model (Abbaspour *et al.* 2017). Based on studies conducted by Rostamian *et al.* (2008), the sequential uncertainty fitting version 2 (SUFI-2) method of SWAT-CUP has good performance in large watersheds. In this study, the SUFI-2 algorithm was employed for the calibration of parameters. The effectiveness of the SWAT model was evaluated employing the coefficient of determination (R^2) and Nush–Sutcliffe efficiency (NSE), these two model efficiency coefficients are calculated based on the following equations (Wang *et al.* 2018):

$$R^2 = \frac{\left[\sum_{i=1}^{n}(O_i - \overline{O})(P_i - \overline{P})\right]^2}{\sum_{i=1}^{n}(O_i - \overline{O})^2 \sum_{i=1}^{n}(P_i - \overline{P})^2} \tag{2}$$

$$\mathrm{NSE} = \frac{\sum_{i=1}^{n}(O_i - \overline{O})^2 - \sum_{i=1}^{n}(P_i - \overline{O_i})^2}{\sum (O_i - \overline{O})^2} \tag{3}$$

In Equations (2) and (3), the observed value is indicated in $\overline{O}$ as the mean value, O_i is the ith of observed value and P_i shows the ith of simulated values, respectively, the mean value of the simulated values shown in $\overline{P}$, and n is the total count of the sample pairs (Wang *et al.* 2018).

While calibrating and validating the model, the selection of parameters is the most time-consuming process to find appropriate parameters that fit the study area and give a satisfactory result. Therefore, the modeller must consider the parameter values for calibrating to reach a very good outcome. The analyst will need to have some experience and knowledge of hydrology to define the initial ranges of the parameters that will be optimized (Abbaspour *et al.* 2007). Local sensitivity (one-at-a-time) and global sensitivity analysis (all-at-a-time (AAT)) are generally the two types of model sensitivity analysis. There is a correlation between parameters in the local sensitivity analysis, that are fully fixed to those worth whose precision is unknown while their simplicity and quickness are the advantages (Abbaspour *et al.* 2017). The parameter ranges and number of runs in the AAT sensitivity analysis undoubtedly have an impact on the relative sensitivity of the parameters, which is considered a form of limitation (Abbaspour *et al.* 2017). Giving reliable results is the advantage of AAT (Abbaspour *et al.* 2017). In this research, sensitive parameters, which are described in Table 1, were selected for model calibration and validation. The sensitivity investigation was carried out using global sensitivity and the resulting list of sensitive parameters was calibrated versus the observed stream discharge data from the general outlet of the Kokcha Watershed (Khwajaghar).

Calibration (2010–2014) and validation (2015–2019) using proper parameters have been done with the coefficient of determination (R^2) as the objective function for both models. 'Global sensitivity analysis is defined by *P*-value and *t*-stat. The larger, in absolute value, the value of the *t*-stat, and the smaller the *P*-value, the more sensitive the parameters' (Abbaspour *et al.* 2017). After determining parameters and their value ranges, model calibration is executed using SWAT-CUP to calibrate the model parameters.

RESULTS AND DISCUSSION

LULC data that are produced by two independent groups can be different in classes and contents. The ESRI LULC data released in 2020 has a 10 m spatial resolution, according to this dataset, the study area is dominated by scrub/shrub. Landsat 8 satellite imagery with 30 m resolution was classified to produce the LULC data for the research area. Based on the classification of Landsat 8, the LULC in the Kokcha Watershed is dominated by bare ground. Landsat 8 was classified into five LULC classes, whereas there are nine LULC types in the ESRI dataset (Figure 2(b)). In Figure 3(a), the natural colour of Landsat 8 (bands 4, 3, and 2) represents a considerable area that is covered by snow. However, in the ESRI LULC data with 10 m resolution, the area is covered by scrub/shrub. This variation between the two datasets can be due to the coarse resolution of Landsat 8, also in the mountainous area, the availability of rocks with white colour could be misidentified as snow. Landsat 8 was downloaded in August 2020, when the temperature of the region states at maximum and the snow/glacier-covered area should be at a minimum.

In the model output using each LULC data, there are some changes in values of average CN, PET, evaporation and transpiration (ET), SF, lateral flow (LF), RF, percolation (Perc), revap from the shallow aquifer (RSA), and recharge to deep aquifers (RDA). The water balance elements correlate with each other and every element is affected by changes in the other components. Table 2 shows the variations in values of elements considering

Table 1 | Parameters and their calibrated values

No	Parameters	Explanation	Fitted value	Min_value	Max_value
1	CN2	SCS runoff CN	9.102	−6.15	11.08
2	ALPHA_BF	Base flow Alpha factor (days)	0.030	0.00	0.06
3	GW_DELAY	Time interval for recharge of the aquifer (days)	46.258	13.94	60.84
4	GWQMN	Threshold depth of water in the shallow aquifer required for RF to occur (mm)	1.334	1.19	1.49
5	OV_N	Manning's 'n' value for overland flow	0.205	0.19	0.22
6	SOL_AWC ()	Available water capacity of the soil layer	0.858	0.77	0.92
7	SURLAG	Delay time of direct SF (days)	10.385	7.18	10.96
8	PPERCO	Phosphorus percolation coefficient	15.949	15.34	16.04
9	SFTMP	[OPTIONAL] Snowfall temperature.	2.351	1.59	3.08
10	SOL_K ()	Saturated soil hydraulic conductivity (mm h − 1)	0.561	0.54	0.78
11	SLSUBBSN	Average slope length (m)	114.546	59.99	120.01
12	HRU_SLP	Average slope steepness	0.218	0.15	0.22
13	ESCO	Soil water evaporation compensation factor (dimensionless)	0.336	0.31	0.52

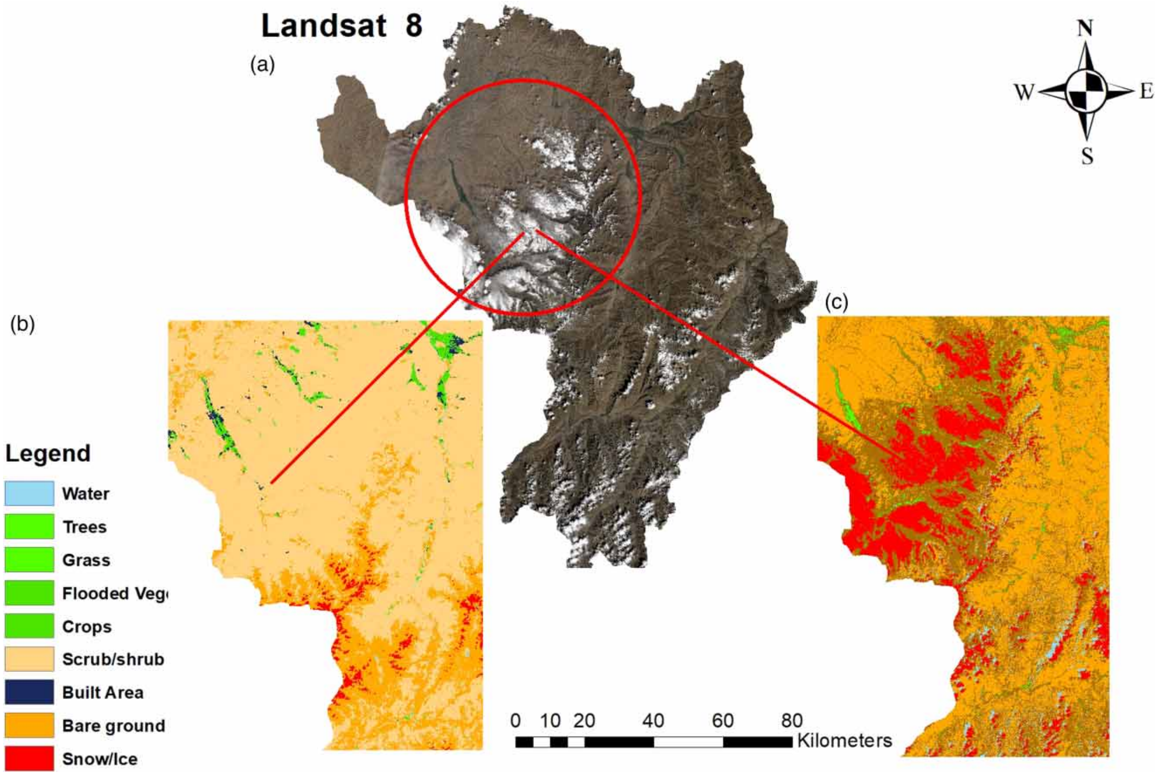

Figure 3 | Changes in identified land cover classes: (a) Landsat 8, natural colour; (b) ESRI LULC; and (c) Landsat 8 LULC.

each of the LULC datasets. For example, the average CN in the model using ESRI LULC data is less than using Landsat 8 data. The less values of CN represent the reduction of runoff in the watershed. The higher values of CN represent a much impervious area in the basin that cause to increase in surface flow. The interrelation among water balance elements is indicated in Table 2. When the average CN decreases from 86.21 to 82.01, the SF drops from 164.26 to 132.75 mm in the Landsat 8 and ESRI data, respectively. Furthermore, PET decreased from 729 to 724.8 mm, whereas ET rose from 161.7 to 167.1 mm using the previously mentioned datasets accordingly.

In the calibration and validation of the model using the ESRI LULC dataset, the most sensitive parameters are GW_DELAY, and ALPHA_BF followed by SFTMP, CN2, and PPERCO. However, based on Landsat 8 LULC data, the five most susceptible parameters are ALPHA_BF, GW_DELAY, SOL_K, HRU_SLP, and SOL_AWC. Figure 4 shows the parameters and selection method of their values in model calibration and validation utilizing the ESRI LULC dataset. Based on the sensitive parameters in the watershed, both LULC datasets represent time intervals for recharge of the aquifer (GW_DELAY) and baseflow alpha factor (ALPHA_BF) as the two most sensitive parameters for runoff generation. The sensitivity of groundwater-related parameters in the area depends on the types of land cover and resolution of LULC datasets in runoff modelling.

The better accuracy of ESRI LULC data can be due to the higher resolution of the dataset, whereas Landsat 8 has a 30 m spatial resolution, and seems complicated to identify each land use class in the small areas. A higher resolution of satellite sensors can differentiate the land cover in mountainous regions that are mostly rocks. However, identifying the changes between rocks with bright colours and snow/ice-covered areas can be challenging

Table 2 | Changes in values of water balance elements

LULC datasets	Average CN	HRUs	PET	ET	SR	LF	RF	Perc	GW
Landsat 8	86.21	464	729	161.7	164.26	28.26	51.82	66.04	17.75
ESRI 2020	82.01	318	724.8	167.1	132.75	28.71	72.17	90.3	19.01

SR, surface runoff.

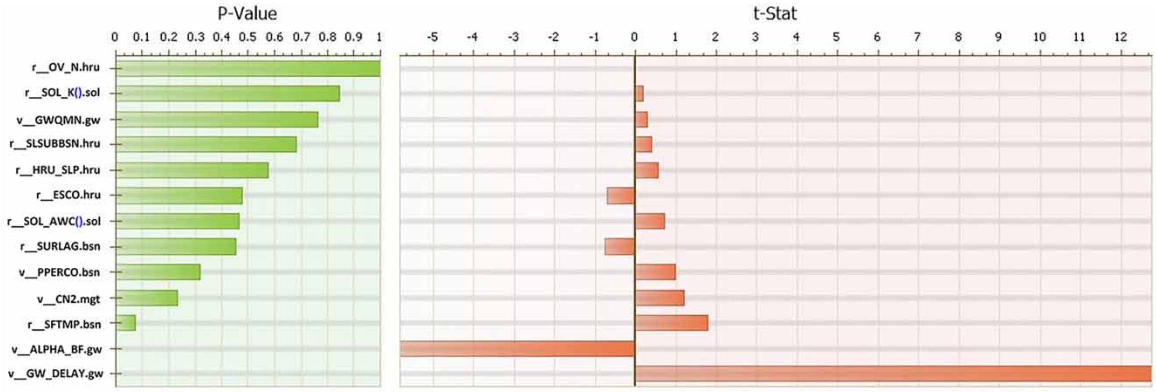

Figure 4 | Sensitive parameters graphical show.

with low-resolution of satellite images. The changes in water balance elements are indicated in Table 2. The most considerable changes between two datasets are in Perc and RF. Higher amount of percolation in the model using the ESRI dataset shows a more permeable area in the watershed, however, utilizing Landsat 8, the permeable regions are less.

The model efficiency coefficient considers both datasets in the calibration and validation of the model range in good class (Table 3). However, the values of the coefficients seem better by utilizing ESRI LULC datasets. Based on the NSE values, which range between 0 and 1, the model using ESRI LULC data in the calibration period gives a 5.5% better result than utilizing LULC data from the classification of Landsat 8. Furthermore, considering the validation period in both LULC datasets, the value of NSE in this period is higher in ESRI than in Landsat 8. The comparison of water balance elements in Table 2 and model efficiency coefficients in Table 3 considering both LULC datasets shows that there is a slight difference between the two datasets in respect of their accuracy. In Table 3, the higher values of R^2 and NSE represent the better compatibility of simulated streamflow to observed river flow. The model outputs from each LULC dataset have been shown in Figures 5 and 6, separately.

Table 3 | Model efficiency coefficient

Datasets		R^2	NSE	P_{BIAS}
Landsat 8	Calibration	0.74	0.64	17.8
	Validation	0.83	0.69	24.5
ESRI 2020	Calibration	0.77	0.70	17.8
	Validation	0.82	0.74	21.0

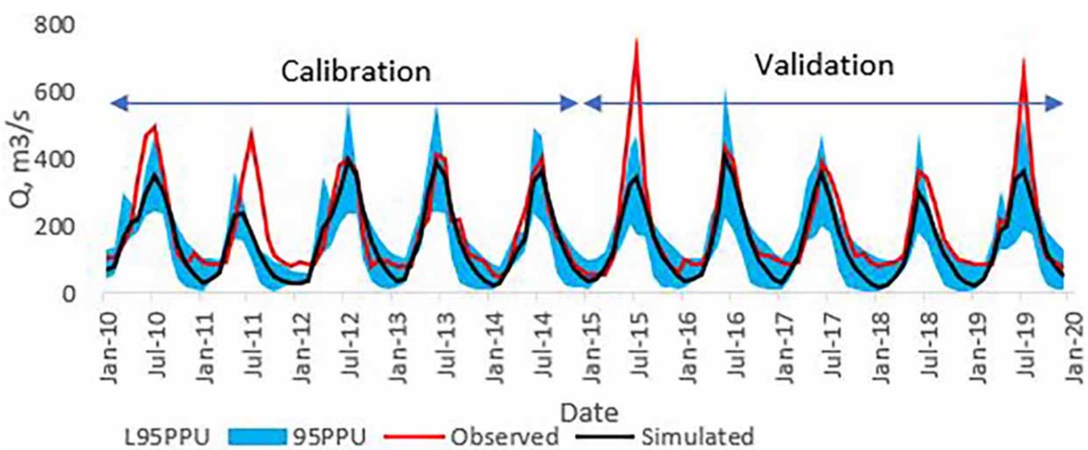

Figure 5 | Model calibration and validation using Landsat 8 LULC data.

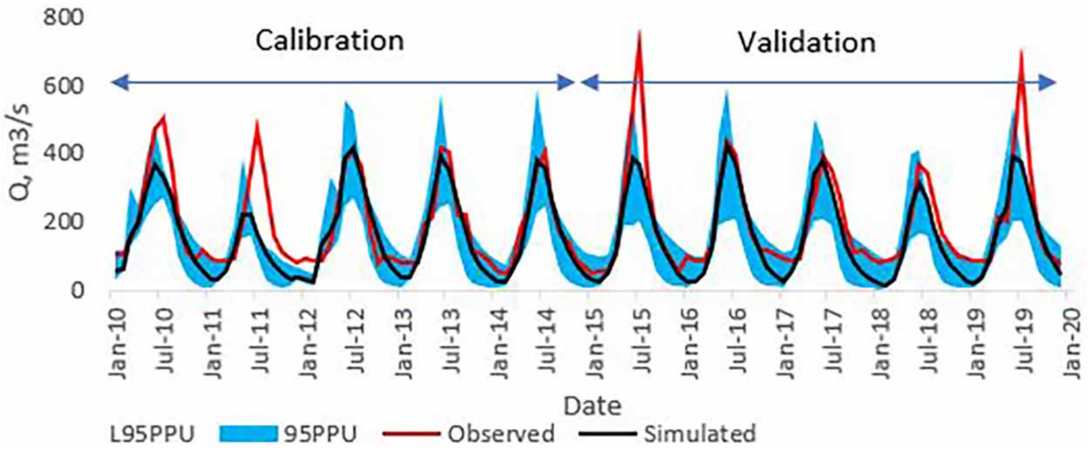

Figure 6 | Model calibration and validation using ESRI 2020 LULC data.

Table 4 | Statistical indices classification

R^2	NSE	P_{BIAS}	Classification
$0.75 < R^2 \leq 1.00$	$0.75 < \text{NSE} \leq 1.00$	$P_{BIAS} \leq \pm 10$	Very good
$0.6 < R^2 \leq 0.75$	$0.6 < \text{NSE} \leq 0.75$	$\pm 10 \leq P_{BIAS} \leq \pm 15$	Good
$0.5 < R^2 \leq 0.6$	$0.5 < \text{NSE} \leq 0.6$	$\pm 15 \leq P_{BIAS} \leq \pm 25$	Satisfactory
$0.25 < R^2 \leq 0.5$	$0.25 < \text{NSE} \leq 0.5$	$\pm 25 \leq P_{BIAS} \leq \pm 50$	Bad
$R^2 \leq 0.25$	$\text{NSE} \leq 0.25$	$\pm 50 \leq P_{BIAS}$	Inappropriate

Source: Adapted from Van Liew *et al.* (2003), Fernandez *et al.* (2005), and Moriasi *et al.* (2007).

In Table 4, the classification of indices is indicated. R^2 in both the calibration and validation of model ranges is in a very good class. However, according to values in NSE, the model matches in good class for both calibration and validation. 'The objective function values classified as very good ($0.75 < R^2 \leq 1$), good ($0.6 < R^2 \leq 0.75$), satisfactory ($0.5 < R^2 \leq 0.6$), bad ($0.25 < R^2 \leq 0.5$) and inappropriate ($R^2 < 0.25$) classes' (Moriasi *et al.* 2007).

As a whole, the result of the model using the LULC data from the ESRI 2020 dataset is slightly better than Landsat 8 LULC data that indicates the accuracy of ESRI LULC data 5.5% more accurate than Landsat 8 LULC data. In this study, all input data were used from remotely sensed sources, which are freely accessible. So, it can be an important reference for hydrological modelling in data-scarce regions.

CONCLUSION

In the situation of the changing climate and population growth, the importance of hydrological modelling is rising continuously. Accurate input data in hydrological modelling is an important issue, however, data scarcity is a big challenge in most parts of the world and in developing countries. This study was assigned to investigate the accuracy of two LULC datasets to indicate how accurate they were for hydrological modelling. The ESRI 2020 global LULC data and the LULC data produced by the classification of Landsat 8 satellite imagery were investigated in this research. Landsat 8 satellite imagery was downloaded in the year 2020. The SWAT model was employed for hydrological modelling. The Penman–Monteith method was considered for PET estimation due to its better performance than the Hargreaves method in the region. The runoff estimation method was selected as SCS-CN and model calibration and validation were performed using SWAT-CUP for both models using each LULC dataset separately.

The obtained results from this research indicated the accuracy of both LULC datasets and the good performance of the SWAT model, whereas the resolutions of the LULC datasets are 10 and 30 m in the ESRI and Landsat 8 datasets, respectively. The accuracy of ESRI global LULC data seems slightly better and gives a 5.5% more precise result than LULC data produced by the classification of Landsat 8 satellite imagery. Identifying urban areas from the Landsat 8 images seems complicated due to the poor urban area of the study region and the low-resolution of Landsat 8. Therefore, it is recommended to use the ESRI 2020 LULC dataset for hydrological modelling using the SWAT model. This research was conducted in the Kokcha Watershed, a semi-arid region located in northern Afghanistan. The methodology used in this study can be applied to other catchments, particularly those located in semi-arid areas with similar topography and environmental characteristics. Due to the significance of LULC data in hydrological modelling and runoff generation, for filling the gap of ground-based data deficiency, it is recommended to conduct similar research using newly released LULC data from remote sensing sources.

ACKNOWLEDGEMENTS

We would like to thank Mr Khan Mohammad Takal head of the National Water Affairs Regulation Authority (NWARA) of Afghanistan for providing ground-based hydro metrological data.

DATA AVAILABILITY STATEMENT

All relevant data are available from an online repository or repositories. (https://drive.google.com/file/d/1Bw-EdTh2vx-1Yck7R2J1Kj9mvwbK-38o/view?usp=share_link).

CONFLICT OF INTEREST

The authors declare there is no conflict.

REFERENCES

Abbaspour, K. C., Yang, J., Maximov, I., Siber, R., Bogner, K., Mieleitner, J., Zobrist, J. & Srinivasan, R. 2007 Modelling hydrology and water quality in the pre-alpine/alpine Thur Watershed using SWAT. *Journal of Hydrology* **333** (2–4), 413–430. https://doi.org/10.1016/j.jhydrol.2006.09.014.

Abbaspour, K. C., Vaghefi, S. A. & Srinivasan, R. 2017 A guideline for successful calibration and uncertainty analysis for soil and water assessment: a review of papers from the 2016 international SWAT conference. *Water (Switzerland)* **10** (1). MDPI AG. https://doi.org/10.3390/w10010006.

Ahady, A. B. & Kaplan, G. 2022 Classification comparison of Landsat-8 and Sentinel-2 data in Google Earth Engine, study case of the city of Kabul. *International Journal of Engineering and Geosciences* **7** (1), 24–31.

Ahmadi, A., Jalali, J. & Mohammadpour, A. 2022 Future runoff assessment under climate change and land-cover alteration scenarios: a case study of the Zayandeh-Roud Dam upstream watershed. Available from: http://iwaponline.com/hr/article-pdf/doi/10.2166/nh.2022.056/1122802/nh2022056.pdf

Almeida, R. A., Pereira, S. B. & Pinto, D. B. F. 2018 Calibration and validation of the SWAT hydrological model for the Mucuri River Basin. *Engenharia Agricola* **38** (1), 55–63. https://doi.org/10.1590/1809-4430-eng.agric.v38n1p55-63/2018.

Althoff, D., Bazame, H. C. & Nascimento, J. G. 2021 Untangling hybrid hydrological models with explainable artificial intelligence. *H2Open Journal* **4** (1). https://doi.org/10.2166/h2oj.2021.066.

Arnold, J. G., Kiniry, J. R., Srinivasan, R., Williams, J. R., Haney, E. B. & Neitsch, S. L. 1998 *Input/Output Documentation Soil & Water Assessment Tool*. Texas Water Resources Institute, TR-439, Texas.

Arnold, J. G., Kiniry, J. R., Srinivasan, R., Williams, J. R., Haney, E. B. & Neitsch, S. L. 2012 *Input/Output Documentation Soil & Water Assessment Tool*. Texas Water Resources Institute, TR-439, Texas.

Chaves, M. E. D., Picoli, M. C. A. & Sanches, I. D. 2020 Recent applications of Landsat 8/OLI and Sentinel-2/MSI for land use and land cover mapping: a systematic review. *Remote Sensing* **12**, 3062. https://doi:10.3390/rs12183062.

Cuceloglu, G., Seker, D. Z., Tanik, A. & Ozturk, I. 2021 Analyzing effects of two different land use datasets on hydrological simulation by using SWAT model. *IJEGEO* **8** (2), 172–185. https://doi.10.30897/ijegeo.828112.

Elachi, C. & van Zyl, J. 2006 Chap 9. In: *Atmospheric Remote Sensing in the Microware Region*. John Wiley & Sons, Inc., pp. 413–443. https://doi.org/10.1002/0471783390.ch9.

Esri 2021. Available from: https://www.esri.com/about/newsroom/announcements/esri-releases-new-2020-global-land-cover-map/

Fernandez, G. P., Chescheir, G. M., Skaggs, R. W. & Amatya, D. M. 2005 Development and testing of watershed-scale models for poorly drained soils. *Transactions of the ASAE* **48** (2), 639–652.

GES DISC 2015 *README Document for the Tropical Rainfall Measurement Mission (TRMM) Version 7*. NASA Goddard Space Flight Center, Code 610.2, Greenbelt, MD 20771, USA. Available from: https://disc2.gesdisc.eosdis.nasa.gov/data/TRMM_L3/TRMM_3B43/doc/README.TRMM_V7.pdf

Getachew, B., Manjunatha, B. R. & Bhat, H. G. 2021 Modeling projected impacts of climate and land use/land cover changes on hydrological responses in the Lake Tana Basin, Upper Blue Nile River Basin, Ethiopia. https://doi.org/10.1016/j.jhydrol.2021.125974.

Hajihosseini, H., Hajihosseini, M., Morid, D. & Booij, M. J. 2016 Hydrological assessment of the 1973 treaty on the transboundary Helmand River, using the SWAT model and a global climate database. *Water Resources Management* **30**, 4681–4694. http://doi.10.1007/s11269-016-1447-y.

Hallouz, F., Meddi, M., Mahé, G., Alirahmani, S. & Keddar, A. 2018 Modeling of discharge and sediment transport through the SWAT model in the basin of Harraza (Northwest of Algeria). *Water Science* **32** (1), 79–88. https://doi.org/10.1016/j.wsj.2017.12.004.

Hussainzada, W. & Lee, H. S. 2021 Hydrological modelling for water resource management in a semi-arid mountainous region using the soil and water assessment tool: a case study in Northern Afghanistan. *Hydrology* **8**, 16. https://doi.org/10.3390/hydrology8010016.

Li, X. H., Zhang, Q. & Xu, C. Y. 2012 Suitability of the TRMM satellite rainfalls in driving a distributed hydrological model for water balance computations in Xinjiang Catchment, Poyang Lake Basin. *Journal of Hydrology* **426–427**, 28–38. https://doi.org/10.1016/j.jhydrol.2012.01.013.

Liu, G., He, Z., Luan, Z. & Qi, S. 2018 Intercomparison of a lumped model and a distributed model for streamflow simulation in the Naoli River Watershed, Northeast China. *Water (Switzerland)* **10** (8). https://doi.org/10.3390/w10081004.

Moriasi, D. N., Arnold, J. G., Liew, M. W. V., Bingner, R. L., Harmel, R. D. & Veith, T. L. 2007 Model evaluation guidelines for systematic quantification of accuracy in watershed simulations. *Transactions of the ASABE* **50** (3), 885–900.

Mwangi, H. M., Julich, S., Patil, S. D., McDonald, M. A. & Feger, K. H. 2016 Relative contribution of land use change and climate variability on discharge of upper Mara River, Kenya. *Journal of Hydrology: Regional Studies* **5**, 244–260. https://doi.org/10.1016/j.ejrh.2015.12.059.

Neitsch, S. L., Arnold, J. G., Kiniry, J. R. & Williams, J. R. 2011 *Soil and Water Assessment Tool Theoretical Documentation Version 2009*.

Nilawar, A. P. & Waikar, M. L. 2018 Use of SWAT to determine the effects of climate and land use changes on streamflow and sediment concentration in the Purna River Basin, India. *Environmental Earth Sciences* **77** (23). https://doi.org/10.1007/s12665-018-7975-4.

Rostamian, R., Jaleh, A., Afyuni, M., Mousavi, S. F., Heidarpour, M., Jalalian, A. & Abbaspour, K. C. 2008 Application of a SWAT model for estimating runoff and sediment in two mountainous basins in central Iran. *Hydrological Sciences Journal* **53** (5), 977–988. https://doi.org/10.1623/hysj.53.5.977.

Sediqi, M. N., Shiru, M. S., Nashwan, M. S., Ali, R., Abubaker, S., Wang, X., Ahmed, K., Shahid, S., Asaduzzaman, M. & Manawi, S. M. A. 2019 Spatio-temporal pattern in the changes in availability and sustainability of water resources in Afghanistan. *Sustainability* **11**, 5836. https://doi:10.3390/su11205836.

Senent-Aparicio, J., Liu, S., Pérez-Sánchez, J., López-Ballesteros, A. & Jimeno-Sáez, P. 2018 Assessing impacts of climate variability and reforestation activities on water resources in the headwaters of the Segura River Basin (SE Spain). *Sustainability (Switzerland)* **10** (9). https://doi.org/10.3390/su10093277.

Serur, A. B. & Adi, K. A. 2022 Multi-site calibration of hydrological model and the response of water balance components to land use land cover change in a rift valley Lake Basin in Ethiopia. *Scientific African* **15**, e01093. https://doi.org/10.1016/j.sciaf.2022.e01093.

Shivhare, N., Dikshit, P. K. S. & Dwivedi, S. B. 2018 A comparison of SWAT model calibration techniques for hydrological modeling in the Ganga River Watershed. *Engineering* **4** (5), 643–652. https://doi.org/10.1016/j.eng.2018.08.012.

Steinhausen, M. J., Wagner, P. D., Narasimhan, B. & Waske, B. 2018 Combining Sentinel-1 and Sentinel-2 data for improved land use and land cover mapping of monsoon regions. *International Journal of Applied Earth Observation and Geoinformation* **73**, 595–604. https://doi.org/10.1016/j.jag.2018.08.011.

US Department of Agriculture 1972 *Soil Conservation Services (USDA-SCS), National Engineering Handbook, Hydrology Section,* Chapters 4–10. USDA, Washington, DC 20250.

Van Liew, M. W., Veith, T. L., Bosch, D. D. & Arnold, J. G. 2003 Suitability of SWAT for the conservation effects assessment project: a comparison on USDA-ARS experimental watersheds. *Journal of Hydrologic Engineering* **12** (2), 173–189.

Venter, Z. S., Barton, D. N., Chakraborty, T., Simensen, T. & Singh, G. 2022 Global 10 m land use land cover datasets: a comparison of dynamic world, world cover, and Esri land cover. *Remote Sensing* **14**, 4101. https://doi.org/10.3390/rs14164101.

Wang, Q., Liu, R., Men, C., Guo, L. & Miao, Y. 2018 Effects of dynamic land use inputs on improvement of SWAT model performance and uncertainty analysis of outputs. *Journal of Hydrology* **563**, 874–886. https://doi.org/10.1016/j.jhydrol.2018.06.063.

Wang, H., Yan, H., Hu, Y., Xi, Y. & Yang, Y. 2022 Consistency and accuracy of four high-resolution LULC datasets – Indochina Peninsula case study. *Land* **11**, 758. https://doi.org/10.3390/land11050758.

Zhou, F., Xu, Y., Chen, Y., Xu, C.-Y., Gao, Y. & Du, J. 2013 Hydrological response to urbanization at different spatio-temporal scales simulated by coupling of CLUE-S and the SWAT model in the Yangtze River Delta region. *Journal of Hydrology* **485**, 113–125. http://dx.doi.org/10.1016/j.jhydrol.2012.12.040.

First received 18 November 2022; accepted in revised form 25 February 2023. Available online 8 March 2023